Casimir interactions in semiflexible polymers

Devin Kachan* and Robijn Bruinsma†
Department of Physics, University of California, Los Angeles, Los Angeles, California 90095-1596, USA

Alex J. Levine‡
Department of Physics, University of California, Los Angeles, Los Angeles, California 90095-1596, USA and Department of Chemistry & Biochemistry and The California Nanosystems Institute, University of California, Los Angeles, Los Angeles, California 90095-1596, USA
(Received 7 August 2012; published 25 March 2013)

We investigate the Casimir or fluctuation-induced interaction between two cross-linkers bound to the same semiflexible filament. The calculation is complicated by the appearance of second-order derivatives in the bending Hamiltonian for such filaments, which requires a careful evaluation of the the path integral formulation of the partition function in order to arrive at the physically correct continuum limit and properly address ultraviolet divergences. Doing so based on the previous work of Kleinert [Kleinert, J. Math. Phys. **27**, 3003 (1986)], we find that cross-linkers interact along a filament with an attractive logarithmic potential proportional to thermal energy. The proportionality constant depends on whether and how the cross-linkers constraint the relative angle between the two filaments to which they are bound. We comment on the implications of this Casimir interaction for equilibrium distribution of labile cross-linkers in semiflexible biopolymer, e.g., F-actin, networks, and bundles.

DOI: 10.1103/PhysRevE.87.032719 PACS number(s): 87.16.Ka, 05.40.−a, 82.35.Lr

I. INTRODUCTION

Objects that modify the fluctuations of their surroundings experience an effective interaction known as the Casimir force after the pioneering work of Casimir [1]. He predicted that two parallel conducting plates separated by a distance D in a vacuum should experience an attractive interaction that decays as $1/D^4$ due to their interaction with the quantum fluctuations of the electromagnetic field. While such Casimir, or fluctuation-mediated, interactions are a general feature of of quantum field theories at zero temperature [2,3], they are also generated by thermal fluctuations in classical systems at finite temperature. In both the thermal and quantum cases, Casimir forces are pronounced in systems with massless modes such as those associated either with broken continuous symmetries (Goldstone modes) in, e.g., liquid crystals [4] or at a critical point (see Refs. [5–7]). Figure 1 demonstrates the Casimir effect schematically: Two plates are held a fixed distance apart in a system with thermally excited Goldstone modes. These fluctuations are represented by the blue ellipses. The boundary conditions imposed by the plates on these soft modes shift their fluctuation spectrum in the region between the two plates in a plate separation-dependent manner. This leads to a contribution to the free energy of the system that now depends on the interplate separation and thereby produces the effective interaction between these objects.

It is tempting to view this thermal Casimir effect as a type of depletion attraction. In this way, thermal fluctuations of wavelength λ are viewed as particles of that size. The effect of bringing the plates together is to exclude the longer wavelength fluctuations or larger particles ($\lambda \geqslant D$) from the region between the fixed plates, resulting in an effective pressure or depletion-type force pushing the plates together. This analogy, while instructive, is not exact, as can be inferred from the observation that the Casimir interaction can be either attractive (as suggested by the above analogy) or repulsive, depending on the boundary conditions imposed on the fluctuations by the embedded objects. The depletion interaction is necessarily attractive. Casimir forces are often obscured by stronger, direct interactions, but not always. For example, the Casimir force between membrane proteins (and other inclusions) due to their modification of the membrane undulations is important because this interaction decays with distance as a power law. In contrast, direct protein-protein interactions are short ranged [8,9].

In this paper we examine Casimir interactions between cross-links on semiflexible polymers. Figure 2 shows an example: Two semiflexible polymers are linked by two sliding linkers. Given linearization of the filament-bending Hamiltonian, we restrict our analysis to cross-linker separations less than a persistence length to ensure that the filament will have only small transverse fluctuations and the arc length will be well parametrized by the projected distance. Fluctuation-induced interactions between cross-linkers in the opposite limit of highly flexible polymers have been studied extensively elsewhere [10,11]. The existence and sign of a Casimir-type force between the linkers can be understood as follows. Imagine that one nails two points along an otherwise free filament. The addition of a fixed point reduces the number of conformational degrees of freedom and hence the entropy. Two fixed points at finite separation result in a further reduction of the number of available states over a single fixed point. The system will therefore find it entropically favorable to place both fixed points at the same position.

The physical interest of this simple model problem lies in possible applications in polymer networks. Thermal fluctuations have long been known to play a central role for the viscoelastic properties of networks of polymers. In particular, the force-extension curve $\tau(D)$ of a polymer of fixed length connecting two points separated by a distance D is believed to determine the elastic properties of the polymer network.

*dkachan@physics.ucla.edu
†bruinsma@physics.ucla.edu
‡alevine@chem.ucla.edu

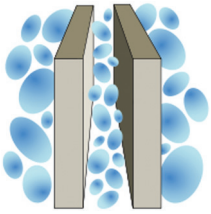

FIG. 1. (Color online) Thermal Casimir effect. As the two plates are brought closer together, fluctuations between the plates are suppressed while the entropy of the surrounding medium increases, resulting in an attractive interaction between the plates.

This force-extension curve is determined largely by thermal fluctuations. There is, however, a fundamental difference between this form of entropic elasticity and the thermal Casimir effect of Fig. 2: If two permanent nodes of a polymer network are brought closer there is no transfer of degrees of freedom from the polymer section between the links to the rest of the network. When the two linkers of Fig. 2 are brought together, degrees of freedom are transferred from the section in between the linkers to the surrounding system. In addition, the computation of the Casimir effect typically requires the regularization of infinities associated with summations over all fluctuation modes. No such divergences appear in the calculation of entropic elasticity. There are interesting examples of biopolymer networks where linker proteins bind reversibly to the protein filaments. Such proteins might exhibit a Casimir interaction due to their modification of the thermally excited transverse undulations of the filaments to which they are bound. A first objection to this idea is that for typical biopolymer networks, the persistence length is much greater than the separation between linkers. On length scales small compared to the persistence length, thermal shape fluctuations must have a low amplitude, so the Casimir interaction is expected to be very weak. Next, biopolymer networks often are under tension, either intrinsic or externally applied. Tension introduces a length scale in the problem beyond which thermal fluctuation are suppressed. In this paper we will demonstrate that the Casimir interaction between sliding linkers on length scales smaller than the persistence length cannot be neglected in networks both with and without tension. We will show that neither effect suppresses the Casimir interaction. Finally, we show that if the linker molecules imposes angular constraints on the filaments at the cross-link, then this generates repulsive elastic stresses, which overwhelm the Casimir interaction. Thus we propose that the distinction between between flexible cross-linkers and stiff ones, associated with filament bundling,

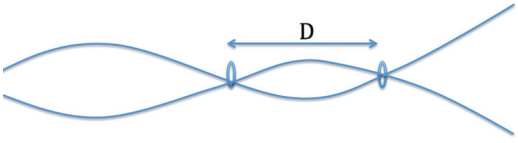

FIG. 2. (Color online) Two semiflexible polymers are linked by two sliding rings. Thermal fluctuations of polymer segments in between the rings are constrained. By reducing the separation D between the rings, the degrees of freedom transferred from in between the rings to the exterior increase the entropy of the system. This generates an attractive interaction between the rings.

has important consequences for the equilibrium distribution of these molecules in semiflexible filament networks.

In Sec. II we discuss the calculation of the partition function that is required for the derivation of the Casimir force. Because of the appearance of higher-order derivatives in the Hamiltonian H, the standard method for evaluating Gaussian functional integrals by path integration is questionable. We will apply a technique introduced by Kleinert [12] for field-theoretic problems to define the integration measure for path integrals with actions that contain higher-order derivatives. In Sec. III we compute the Casimir interaction using this functional integral technique and examine a few cases. In Sec. IV we review our results in the context of polymer networks.

II. PARTITION FUNCTION

A. Model Hamiltonian

Let two linkers be separated by a distance D along the z axis. A semiflexible polymer of bending modulus κ and thus persistence length $l_p = \beta\kappa \gg D$ is threaded through the two linkers. Here and throughout $\beta = \frac{1}{k_B T}$. The cross-linkers fix the position and direction of the polymer at the linker locations, but the length of the polymer between the linkers is not fixed. This corresponds to the case of Fig. 2 if one of the two polymers is subject to a very strong tension. Since we do not consider the steric interaction between the filaments, the Casimir force for Fig. 2 is then simply twice the force computed below.

We specify the filament configuration by its (two-dimensional) displacement $\vec{h}(z)$ from the z axis and neglect torsional and compressional modes of the filament in order to write its thermal partition function as

$$\mathcal{Z} = \int \mathcal{D}\vec{h}(z)\, e^{-\beta\mathcal{H}[\vec{h}]}. \tag{1}$$

For $D \ll l_p$, so that this partition sum is dominated by nearly straight configurations of the filament, the elastic energy $\mathcal{H}$ can be expressed in terms of $\vec{h}(z)$ as

$$\mathcal{H}\{\vec{h}\} \approx \frac{1}{2}\int_0^D dz\left[\kappa\left(\frac{d^2\vec{h}(z)}{dz^2}\right)^2 + \tau\left(\frac{d\vec{h}(z)}{dz}\right)^2\right], \tag{2}$$

in the so-called small gradient approximation. The first term gives the contribution to filament curvature, while the second term accounts for a tension τ applied to the polymer. Because the polymer can freely slide through the linkers, the linkers do not absorb this tension. However, the two linkers do impose the local boundary conditions on the displacement $\vec{h}(z=0) = \vec{h}(z=D) = 0$ and direction $\vec{h}'(z=0) = \vec{v}_a, \vec{h}'(z=D) = \vec{v}_b$ of the polymer. These boundary conditions correspond to perfect pinning cross-linkers, i.e., ones that can provide arbitrary constraint forces to fix the filament's position perfectly. In any physical biopolymer system, however, the cross-linking molecules have some finite elastic compliance and are of finite size. Such molecules cannot precisely pin the filament at a point. The use of perfect cross-linkers allows one to better isolate the role of filament fluctuations on the Casimir interaction of two cross-linkers. Corrections associated with a finite elastic compliance are explored in the discussion

following Eq. (47). The finite size of the cross-linkers may be considered within our framework by modeling them as rings that enforce the boundary conditions only when the filament's transverse displacement becomes larger than the rings' radius (see Fig. 2). For the Casimir effect to be operative between two such ringlike cross-linkers, one must be sure that the scale of transverse undulations at a location on the filament without a cross-linker is larger than the ring radius. Larger rings would have no effect on the filament's fluctuation spectrum and thus generate no Casimir interaction.

The scale of the transverse undulations of a semiflexible filament may be estimated using equipartition. The mean square height fluctuations in equilibrium are proportional to k_BT/κ, i.e., they are inversely proportional to the persistence length. Dimensional analysis gives the remaining dependence on the filament length L so that the characteristic scale of the height fluctuations is $\langle h^2\rangle \sim L^3/l_p$, as noted previously by others [13]. Such transverse fluctuations in F-actin have been well studied experimentally (see, e.g., Ref. [14]). We present a more thorough analysis in Appendix C, where we determine the scale of fluctuations at a given distance away from a cross-linker. Based on this analysis in Appendix C, we find that Casimir interactions should be present between nanometer-scale binding proteins down to cross-linker separations of ~10 nm for F-actin. Below that short distance two cross-linkers will experience a rapidly diminishing attractive interaction. On stiffer filaments this cutoff will be larger, as discussed in Appendix C.

Within the small gradient approximation, it is clear that the two transverse polarizations $h_{x,y}(z)$ of the filament undulations decouple, so the resulting partition sum is simply the product of two copies of the partition sum over a scalar field $h(z)$ representing one transverse mode, but still obeying the Hamiltonian equation (2). To absorb the bending modulus, it is convenient to rescaled lengths $z = (\beta\kappa)^{1/3}\tilde{z} = l_p^{1/3}\tilde{z}$. Finite tension introduces a length scale, which we write in terms of a wave number $q = (\beta\tau/l_p^{1/3})^{1/2}$. We note that the rescaled length $\tilde{z}$ has physical dimensions of $L^{2/3}$; q has dimensions of inverse $\tilde{z}$. After this change of independent variables, the filament Hamiltonian reduces to

$$\mathcal{H} = \frac{1}{2}\int_0^D dz[h''(z)^2 + q^2h'(z)^2]. \tag{3}$$

Here and in the remainder we remove the tildes from all rescaled lengths and we measure energies in units of β^{-1}.

In analogy to the standard presentation of the path integral approach to quantum mechanics classical, we decompose the field $h(z)$ in terms of the classical solution $h_{\rm cl}(z)$, which minimizes the energy, and the fluctuations around it, writing

$$h(z) = h_{\rm cl}(z) + \delta h(z). \tag{4}$$

The stationarity condition $\frac{\delta\mathcal{H}}{\delta h} = 0$, which imposes the force balance condition for a flexible beam, requires the classical trajectory to satisfy the differential equation

$$h_{\rm cl}'''' - q^2h_{\rm cl}'' = 0. \tag{5}$$

We require the classical solution to satisfy the appropriate boundary conditions at the end points $z = 0$ and D. By choosing the appropriate coordinate system, we may always set $h(0) = h(D) = 0$. We define the initial and final tangents to be $h'(0) = v_a$ and $h'(D) = v_b$. The fluctuation field $\delta h(z)$ and its first derivative are required to vanish at the end points. The general solution of Eq. (5) is

$$h_{\rm cl}(z) = a\sinh qz + b\cosh qz + cz + d, \tag{6}$$

with undetermined constants a, b, c, and d.

Using the decomposition equation (4) and integrating by parts, one finds that the energy of a configuration separates into a classical path contribution and one from the fluctuations about that path: $\mathcal{H} = \mathcal{H}_{\rm cl} + \mathcal{H}_{\rm fl}$. The energy associated with the classical trajectory is given solely by the boundary term:

$$\mathcal{H}_{\rm cl} = \tfrac{1}{2}[h_{\rm cl}''h_{\rm cl}' - h_{\rm cl}'''h_{\rm cl} + q^2h_{\rm cl}'h_{\rm cl}]\big|_{h'(0)=v_a}^{h'(D)=v_b}. \tag{7}$$

Due to our choice of the initial and final values of $h_{\rm cl}$, only the first term makes a nonvanishing contribution to the elastic energy of the bent filament. Applying the boundary conditions to set the undetermined constants in Eq. (6), we find the energy of the classical trajectory to be

$$\mathcal{H}_{\rm cl} = \frac{1}{2}\frac{q\big(qD\big(v_a^2+v_b^2\big)\cosh(qD) - (v_a-v_b)^2\sinh(qD) - 2qDv_av_b\big)}{2[1-\cosh(qD)] + qD\sinh(qD)}. \tag{8}$$

The above result reduces to a particularly simple form in the limit of zero tension $q = 0$. There the elastic energy of the filament depends on the initial and final tangents through the expression

$$\mathcal{H}_{\rm cl} = \frac{2l_pk_BT}{D}\big(v_a^2 + v_b^2 + v_av_b\big), \tag{9}$$

in the original units. In response to choosing symmetric imposed tangent angles $v_a = -v_b = \theta/2$ and defining a radius of curvature R via $\theta = D/R$, the energy-minimizing filament trajectory is an arc of a circle with radius R and the stored elastic energy is $\frac{\kappa D}{2R^2}$ (in the original units), as expected. This solution is shown in Fig. 3. Of course, for much larger bends, where the replacement of the curvature by the second derivative in the Hamiltonian is inappropriate, a more

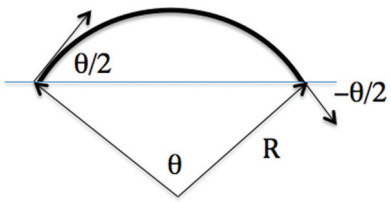

FIG. 3. (Color online) Elastic rod subject to a torque is bent into the shape of a circular arc. The radius of curvature of the arc is R and the angle subtending the arc is θ.

complicated solution is obtained involving elliptic functions [15]. The remaining part of the partition function involves the integral over all allowed fluctuations

$$\mathcal{Z} = e^{-\mathcal{H}_{\rm cl}} \int \mathcal{D}\delta h(z) e^{-\beta \mathcal{H}_{\rm fl}\{\delta h\}}, \tag{10}$$

where

$$H_{\rm fl}\{\delta h\} = \frac{1}{2}\int_0^D dz[\delta h''(z)^2 + q^2 \delta h'(z)^2], \tag{11}$$

where δh and its derivative must vanish at both ends of the filament.

B. Naïve mode analysis: Casimir force and force extension relation

To evaluate the functional integral, one slices the spatial coordinate z into $N+1$ pieces of width ϵ such that $z_n = \epsilon n$ and $\epsilon(N+1) = D$. In this approach ϵ plays the role of a short-distance cutoff for the continuum theory. For polymers one typically imagines this length to be related to the monomer size. For the continuum approach to be meaningful, physical quantities such as the Casimir force should not depend on the precise formulation of this cutoff. In contrast, extensive thermodynamic properties, such as the heat capacity, necessarily depend on the number of degrees of freedom and thus retain an ϵ dependence. With this slicing of the functional integral, we may replace the measure by

$$\mathcal{D}h = \prod_{n=1}^{N} \int_{-\infty}^{\infty} \frac{dh_n}{\Delta h}, \tag{12}$$

where Δh is a phase factor with dimension of length. The partition function of the segment can be evaluated by expanding the fluctuation displacement into a series of harmonic modes

$$h_n = \sqrt{\frac{2}{3(N+1)}} \sum_{m=1}^{N} A_m[\cos(k_m z_n) - 1], \tag{13}$$

with wave number $k_m = 2\pi m/D$. The normalization of the harmonic modes in Eq. (13) has been chosen so as to set the Jacobian of the transformation to unity. The calculation of the remaining Gaussian integrals is straightforward. The answer can be inferred directly by noting that the energy stored in the mth mode in thermal equilibrium is

$$U_m = \frac{\epsilon}{4}\left(\kappa k_m^4 + \tau k_m^2\right) A_m^2 \tag{14}$$

(in the original units), which is the energy of a harmonic oscillator having spring constant $K_m = \frac{\epsilon}{2}(\kappa k_m^4 + \tau k_m^2)$. Since these harmonic modes are decoupled, the free energy of the N modes with spectrum $\omega(k_m) \propto \sqrt{K_m}$ is given by the sum

$$\Delta F(D) = k_B T \sum_{m=1}^{N} \ln[\Gamma \omega(k_m)/k_B T] \tag{15}$$

of their free energies. Here Γ is a phase-space factor that does not depend on D. Converting the summation to an integration, we write

$$\Delta F(D)/k_B T = \frac{D}{2\pi}\int_{2\pi/D}^{2\pi/\epsilon} \ln[\Gamma \omega(k)/k_B T] dk. \tag{16}$$

At zero tension this reduces to

$$\Delta F(D)/k_B T = D \ln\left(\frac{\Gamma \epsilon \kappa}{k_B T}\right)^{1/2}\left(\frac{1}{\epsilon} - \frac{1}{D}\right) + 2D\left(\frac{1}{\epsilon}\ln(2\pi/\epsilon) - \frac{1}{D}\ln(2\pi/D) - \frac{1}{\epsilon} + \frac{1}{D}\right). \tag{17}$$

To compute the Casimir force between the cross-links, we must include the section of the filament outside of them. We consider a filament of total length $L \gg D$. To avoid additional complexities associated with the choice of boundary conditions at the free ends, we assume the filament to be linked into a loop. Then the total free energy of the loop with two cross-links is $F_T(D) = \Delta F(D) + \Delta F(L-D)$. The Casimir force $-dF_T(D)/dD$ is then $f_C(D) = f(D) - f(L-D)$, where we have defined $f(D) = -d\Delta F(D)/dD$. Each of the two fluctuation-induced interactions between the linkers takes the form

$$f(D)/k_B T = -\ln\left(\frac{\Gamma(\epsilon\kappa)^{1/2}}{k_B T}\right)\frac{1}{\epsilon} - 2\left(\frac{1}{\epsilon}\ln(2\pi/\epsilon) + \frac{1}{D} - \frac{1}{\epsilon}\right). \tag{18}$$

This expression must be proportional to an inverse length. The system has three characteristic lengths: the persistence length (which is proportional to the bending modulus κ), the short-distance cutoff ϵ, and D. We note that the force depends on all three in a manner such that it diverges in the continuum limit $\epsilon \to 0$. However, after the subtraction of the two fluctuation-induced interactions within the loop, each divergent in the $\epsilon \to 0$ limit, the residual Casimir force is finite and in the limit $L \gg D$ is given by

$$f_C(D) \approx \frac{-4k_B T}{D}, \tag{19}$$

where, recalling the two independent undulatory polarization states, we have multiplied our result by 2. This expression has a universal character: It is independent of the short-distance cutoff, the persistence length, or the phase factor. To estimate the magnitude of this force in typical biopolymer systems, we note that at a separation of 10 nm, the attractive force is on the order piconewtons, the typical force scale of motor proteins. The work required to separate the two cross-links from 100 nm to 1 μm is $\sim 9k_B T$. If the tension term were kept, then the Casimir force would be unchanged for inter-cross-link separations of $D < 1/q$, but would be reduced by a factor of 2 for larger separations $D \gg 1/q$.

It is essential to recognize that the finite Casimir force between the two cross-linkers on the loop was produced by the subtraction of the two fluctuation-induced interactions, each of which diverged in the continuum limit of $\epsilon \to 0$. The naive mode analysis is not capable of separating the finite Casimir force from these cutoff-dependent terms, which diverge in the continuum limit. Although this result is shown for the case of a filament at zero tension, the same issue appears for all finite tension. That tension, of course, can be employed as a Lagrange multiplier in order to fix the mean arc length of the filament. Controlling mean length in this way does not eliminate the divergences associated with naive mode analysis.

Of course, physical polymers have a natural short-distance cutoff related to their monomer size. By fixing ϵ the naive mode analysis gives the free energy of a polymer of $N = D/\epsilon$ degrees of freedom. The variation of that free energy with length D (necessary to calculate the Casimir force) changes the total number of degrees of freedom, making the analysis of the problem complicated. This procedure gives a Casimir force with cutoff-dependent contributions. The precise nature of the cutoff, however, should not determine the physical force between distant pinning sites on the polymer. The subtraction scheme used above masks our ignorance by subtracting this cutoff dependence and is able to reproduce the correct Casimir force, but it is not inherently satisfactory. The path integral method outlined in Sec. II C systematically arrives at a free energy that neatly separates cutoff-dependent divergences and in this way produces an explicitly finite Casimir force in the limit of $\epsilon \to 0$.

As mentioned, the appearance of divergences is a signature of calculations of the Casimir force [4]. More care must be used in taking the continuum limit in the Casimir force calculation than is generally necessary in computing other physical quantities associated with semiflexible filaments. For example, one may compute the force-extension curve of such a filament and take the continuum limit without encountering the infinities discussed above. We review that calculation briefly.

Including a finite tension on the filament, we may compute the thermal expectation values of the squared amplitudes [see Eq. (13)] of the various undulatory fluctuations on the filament. Using the equipartition theorem and Eq. (14), we immediately obtain

$$\langle A_m^2 \rangle = \frac{2}{\epsilon}\left(k_m^4 + q^2 k_m^2\right)^{-1}. \tag{20}$$

The arc length L of the filament between two points separated by D is

$$L = \int_0^D dz \sqrt{1 + h'(z)^2}, \tag{21}$$

where we again consider only one polarization state for the fluctuations. Using Eqs. (20) and (21), we find the mean arc length between those points to be given by

$$L/D - 1 \propto \frac{1}{D}\sum_{m=1}^{D/\epsilon}\left(k_m^2 + q^2\right)^{-1}. \tag{22}$$

The key observation is that the summation converges in the limit $\epsilon \to 0$. In that continuum limit, changing from summation to integration leads to the force-extension relation $L/D - 1 \propto 1/\tau^{1/2}$ for semiflexible polymers in the limit of high tensions. This is a well-known result that has been verified by micromechanical experiments [16].

The appearance of infinities in the Casimir force calculation raises questions as to the reliability of our result, as it is far from clear that our procedure properly separates the divergent and nondivergent terms. In contrast, the force-extension calculation, as presented above, does not suffer from these infinities and consequently should be considered to be more reliable. The source of our difficulties lies in the free energy [Eq. (17)], where the dependence on D and ϵ is mixed together. A related problem concerns the fact that the Hamiltonian contains higher-order derivatives. In a standard Feynman-type evaluation of a functional integral over all possible trajectories, analytical functions such as $h(z)$ are replaced by a piecewise linear function that interpolates between the values $h(z_i)$ evaluated at adjacent slices z_i separated along the z axis by the short-distance cutoff ϵ. In a Hamiltonian that contains only first derivatives, these are replaced by $[h(z_{i+1}) - h(z_i)]/\epsilon$. Physically meaningful results are then obtained for the functional integral in the limit that the width of the slice goes to zero. If, however, the Hamiltonian contains higher-order derivatives, as in the present case, then approximating $h(z)$ by a piecewise linear interpolation leads to ambiguities. Curvature energies, for example, would be infinite at the cusps of a piecewise linear trajectory. Replacing the curvature by a discrete second derivative avoids this divergence, but that introduces interactions between time slices that are not adjacent, with mathematically unclear consequences. In the following section we will present a method for computing the Casimir force that avoids the ambiguities of the naive method.

C. Kleinert functional integral

We will use a method introduced by Kleinert [12] in the context of field theories with actions that contain higher-order derivatives. A higher-dimensional functional integral will be evaluated that contains only first derivatives. This Kleinert functional integral can be computed without ambiguity by the usual Feynman method. The result does not depend on the short-distance cutoff. In the present case, we need to establish a relation between the Kleinert functional integral and the partition function that we want to calculate.

The Kleinert functional integral is

$$\mathcal{Z}_K = \int \mathcal{D}h\mathcal{D}v\mathcal{D}p\mathcal{D}p_v \times \exp\left\{\int dz\left[ip(h' - v) + ip_v v' - \frac{1}{2}\left(p_v^2 + q^2 v^2\right)\right]\right\}. \tag{23}$$

If one were to drop the first two terms of the argument of the exponential, the functional integral would resemble the path integral expression of the density matrix of a quantum harmonic oscillator, with p_v playing the role of the canonical momentum. It should be kept in mind that in classical statistical mechanics momentum integration produces the partition function of the ideal gas. The variable p_v is only a mathematical aid and should not be viewed as a physical momentum variable.

The relation with the partition function that we want to compute can be seen intuitively by completing the square of $p_v(z)$ in the Kleinert Hamiltonian. This produces a term $-\frac{1}{2}v'(z)^2$ inside the square brackets. Next the functional integral over $p(z)$ produces a δ function at every time slice. That imposes the condition $h'(z_i) = v_i$, which transforms $v'(z)$ into a discretized version of $h''(z)$. After performing the functional integrals over p, p_v, and $h' = v$, the remaining functional integral over $h(z)$ is expected to be proportional to the partition function. We must carefully verify, however, that the multiplicative constant does not involve any dependence on D.

To explicitly evaluate the functional integral, slice the spatial coordinate z into $N+1$ pieces of width ϵ such that $z_n = n\epsilon$ and $(N+1)\epsilon = D$. The boundary conditions translate into the requirements

$$h_0 = 0, \quad h_{N+1} = 0, \quad v_1 = v_a, \quad v_{N+1} = v_b. \tag{24}$$

There are no boundary conditions imposed on p and p_v. A piecewise linear path is now defined by the values of (h_n, v_n, p_n, p_{v_n}) at each slice, with a straight line path in four-dimensional phase space interpolating between adjacent slices. Since the phase-space coordinates are independent, we recover all possible paths by integrating over each variable at each slice. The measures $\mathcal{D}h, \mathcal{D}v, \mathcal{D}p$, and $\mathcal{D}p_v$ in the partition function are defined to be

$$\begin{aligned} \mathcal{D}h &= \prod_{n=1}^{N} \int_{-\infty}^{\infty} \frac{dh_n}{\Delta h}, \quad \mathcal{D}v = \prod_{n=2}^{N} \int_{-\infty}^{\infty} \frac{dv_n}{\Delta v}, \\ \mathcal{D}p &= \prod_{n=1}^{N+1} \int_{-\infty}^{\infty} \frac{dp_n}{2\pi\,\Delta p}, \quad \mathcal{D}p_v = \prod_{n=2}^{N+1} \int_{-\infty}^{\infty} \frac{dp_{v_n}}{2\pi\,\Delta p_v}. \end{aligned} \tag{25}$$

The factors Δh, Δv, Δp, and Δp_v are included in the definition of the elementary volume in the four-dimensional phase space to construct a partition function that is dimensionless, just as a factor with the dimensions of $\hbar^3$ must be included in the partition function of classical systems. The phase-space factors can be combined into the term $\Delta^{-N} = \Delta h^{-N} \Delta v^{-N+1} \Delta p^{-N-1} \Delta p_v^{-N}$.

All first-order derivatives in the Hamiltonian can be discretized:

$$\begin{aligned} \tilde{\mathcal{H}} = \epsilon \sum_{n=1}^{N+1} \Bigg[&-ip_n \left(\frac{h_n - h_{n-1}}{\epsilon} - v_n \right) - ip_{v_n} \left(\frac{v_n - v_{n-1}}{\epsilon} \right) \\ &+ \frac{1}{2} \left(p_{v_n}^2 + q^2 v_n^2 \right) \Bigg]. \end{aligned} \tag{26}$$

First, perform the Gaussian integrals over p_{v_n}. This gives one factor $(2\pi\epsilon)^{-1/2}$ for every n and a term $\frac{1}{2}(\frac{v_n - v_{n-1}}{\epsilon})^2$ inside the square brackets. Next perform the integrals over p_n. This produces one δ function $\delta(h_n - h_{n-1} - \epsilon v_n)$ for every n. Finally, the integrals over v_n combined with the δ function means replacing v_n by $\frac{h_n - h_{n-1}}{\epsilon}$. Finally, a factor of $1/\epsilon$ is generated by each of the $N-2$ integrals over v_n through the δ functions. The final result is

$$\mathcal{Z}_K = \frac{1}{\epsilon^{3N/2-1}} \left[\prod_{n=1}^{N} \int_{-\infty}^{\infty} \frac{dh_n}{\Delta} \right] \delta(h_N - \epsilon v_b) \delta(h_1 - \epsilon v_a) e^{-\mathcal{H}}, \tag{27}$$

where the Hamiltonian is given by

$$\mathcal{H} = \frac{\epsilon}{2} \sum_{n=1}^{N} [(\nabla \bar{\nabla} h_n)^2 + q^2 (\nabla h_n)^2]. \tag{28}$$

Here ∇ and $\bar{\nabla}$ are the forward and backward lattice derivatives

$$\nabla h(z) = \frac{h(z+\epsilon) - h(z)}{\epsilon}, \quad \bar{\nabla} h(z) = \frac{h(z) - h(z-\epsilon)}{\epsilon}. \tag{29}$$

Equation (27) provides us with the desired relation between the Kleinert functional integral and the partition function. The latter is $\mathcal{Z}_K$ without the prefactor $\epsilon^{-3N/2+1}$ and with Δ replaced by a suitable Δh that makes the partition function dimensionless. Note that $h(z)$ in the functional integral is here allowed to have a slope at the end points that differs from the imposed boundary condition with the boundary condition enforced by the two δ functions.

D. Partition function

To explicitly compute $\mathcal{Z}_K(\epsilon)$, it is convenient to leave the integral over p_1 and p_{N+1} in place. As before, we separate the displacement into a classical and a fluctuation part. The classical contribution $\mathcal{Z}_{\rm cl} = e^{-\mathcal{H}_{\rm cl}(v_a, v_b)}$ is given by Eq. (7), just as in the naive mode analysis. Carry out a mode analysis by expanding the displacement in a sine series:

$$\delta h(z) = \sqrt{\frac{2}{N+1}} \sum_{m=1}^{N} A_m \sin k_m z, \tag{30}$$

with $k_m = \frac{m\pi}{D}$. This decomposition differs from that of the naive mode analysis in that the sine series imposes only the zero displacement boundary conditions $h_0 = h_{N+1} = 0$ at the ends, but does not constrain the angles there. The remaining boundary conditions on the angles are imposed afterward through the integral over p_1 and p_{N+1}. The fluctuation part of the Kleinert Hamiltonian is

$$\mathcal{H}_{\rm fl} = \frac{\epsilon}{2} \sum_{m=1}^{N} \left(Q_m^4 + Q_m^2 q^2 \right) A_m^2. \tag{31}$$

Here

$$Q_m^2 = \frac{2 - 2\cos(k_m \epsilon)}{\epsilon^2} \tag{32}$$

is the mode dispersion relation of a linear chain. Equation (30) is an orthogonal transformation with unit Jacobian.

Finally, we express δh_1 and δh_N in $\exp\{ip_1 \delta h_1 - ip_{N+1} \delta h_N\}$ in terms of the sine series

$$\begin{aligned} &\exp\{ip_1 \delta h_1 - ip_{N+1} \delta h_N\} \\ &\quad = \exp\left\{ i\sqrt{\frac{2}{N+1}} \left[(p_1 - p_{N+1}) \sum_{m\ \text{odd}}^{N} A_m \sin(k_m \epsilon) \right.\right. \\ &\qquad \left.\left. + (p_1 + p_{N+1}) \sum_{m\ \text{even}}^{N} A_m \sin(k_m \epsilon) \right] \right\}. \end{aligned}$$

The functional integral over the fluctuations, after the change of variables, is then

$$\begin{aligned} \mathcal{Z}_{\rm fl} = \epsilon \Delta^{-N} &\prod_{m=1}^{N} \left[\int_{-\infty}^{\infty} \frac{dA_m}{\sqrt{2\pi\epsilon}\epsilon} \right] \int_{-\infty}^{\infty} \frac{dp_1}{2\pi} \int_{-\infty}^{\infty} \frac{dp_{N+1}}{2\pi} \\ &\times \exp\left\{ i\sqrt{\frac{2}{N+1}} \left[(p_1 - p_{N+1}) \sum_{m\ \text{odd}}^{N} A_m \sin(k_m \epsilon) \right.\right. \\ &\left.\left. + (p_1 + p_{N+1}) \sum_{m\ \text{even}}^{N} A_m \sin(k_m \epsilon) \right] \right\} \\ &\times \exp\left\{ \frac{\epsilon}{2} \sum_{m=1}^{N} \left(Q_m^2 + q^2 \right)^2 A_m^2 \right\}. \end{aligned} \tag{33}$$

The integrals over the mode amplitudes A_m are Gaussian. Evaluation produces the product of a prefactor

$$\prod_{m=1}^{N}\left(\epsilon^2 Q_m^2+\epsilon^2 q^2\right)^{-1} \tag{34}$$

that includes a factor $\frac{1}{\sqrt{2\pi\epsilon\epsilon}}$ and a piece that depends on p_1 and p_{N+1}:

$$\int_{-\infty}^{\infty}\frac{dp_1}{2\pi}\int_{-\infty}^{\infty}\frac{dp_{N+1}}{2\pi}\exp\left\{-\frac{1}{(N+1)\epsilon}[(p_1-p_{N+1})^2\Sigma_o +(p_1+p_{N+1})^2\Sigma_e]\right\}, \tag{35}$$

where

$$\Sigma_{e,o}=\sum_{\substack{m\,\text{even}\\ m\,\text{odd}}}^{N}\frac{\sin^2(k_m\epsilon)}{\left(Q_m^2+q^2\right)^2}. \tag{36}$$

The infinite product [Eq. (34)] and the sums $\Sigma_{e,o}$ can be evaluated in the limit $N\to\infty$ giving

$$\Sigma_e=\frac{\epsilon^2 D}{8q}\coth\left(\frac{qD}{2}\right),\quad \Sigma_o=\frac{\epsilon^2 D}{8q}\tanh\left(\frac{qD}{2}\right) \tag{37}$$

(see Refs. [17,18]). The remaining momenta integrals [Eq. (35)] are Gaussian. After evaluation and combination with Eq. (34), the fluctuation contribution to the partition function is

$$\mathcal{Z}_{\rm fl}=\frac{1}{2\pi\,\Delta^N}\frac{q^2}{\sqrt{2(1-\cosh qD)+qd\sinh qD}}. \tag{38}$$

The final result for the Kleinert functional integral

$$\mathcal{Z}_K=e^{-\mathcal{H}_{\rm cl}}\frac{1}{2\pi\,\Delta^N}\frac{q^2}{\sqrt{2(1-\cosh qD)+qd\sinh qD}} \tag{39}$$

does not depend on the short-distance cutoff. The actual partition function

$$\mathcal{Z}=e^{-\mathcal{H}_{cl}}\frac{\epsilon}{2\pi(\epsilon^{3/2}\Delta)^N}\frac{q^2}{\sqrt{2(1-\cosh qD)+qd\sinh qD}}, \tag{40}$$

however, does depend on the short-distance cutoff, but only through a multiplicative constant, which can be absorbed into the phase factor. The free energy equals

$$\frac{\mathcal{F}}{k_BT}=\mathcal{H}_{\rm cl}-\ln\left(\frac{q^2}{\sqrt{2(1-\cosh qD)+qD\sinh qD}}\right) +N\ln\sqrt{\frac{\Delta^2\epsilon^3}{k_BT}}-\ln(\epsilon/2\pi). \tag{41}$$

The first term, the classical Hamiltonian, is the elastic energy of the chain in the absence of thermal fluctuations. It is of course independent of the microscopic cutoff. The second term is also independent of the short-distance cutoff and will be the source of the Casimir force. The third term, which depends explicitly on the cutoff, is extensive in the number N of microscopic degrees of freedom and dominates in the large-N limit. Now the finite and divergent terms are cleanly segregated in the free energy: The dependence on the short-distance cutoff, which stands for the dependence on microscopic variables, appears only in the free energy per monomer.

Note that, unlike the case of field theory whose methods we have been using here, there is nothing unphysical in the remaining dependence of the free energy on the microscopic cutoff. In fact, $-T\frac{\partial^2 F}{\partial T^2}$ must equal the Dulong-Petit heat capacity $\frac{N}{2}k_B$ in the limit of large N according to classical statistical mechanics. The third term (with the explicit temperature dependence restored) ensures that this relation holds even as ϵ is taken to zero.

III. LINKER INTERACTION POTENTIAL

We can now use the results of the preceding section to infer the effective interaction between sliding linker molecules. We start with the case of zero tension when the partition function reduces to

$$\mathcal{Z}\propto\frac{1}{D^2}e^{-(2/D)(v_a^2+v_b^2+v_av_b)} \tag{42}$$

and the free energy

$$\mathcal{F}=-k_BT\ln\mathcal{Z} =k_BT\left(2\ln\tilde{D}+\frac{2}{\tilde{D}}\left(\tilde{v}_a^2+\tilde{v}_b^2+\tilde{v}_a\tilde{v}_b\right)\right)+C. \tag{43}$$

The constant C, which is independent of D and the boundary conditions, plays no further role. The tildes have been reinserted here as a reminder: $\tilde{D}=l_p^{-1/3}D,\tilde{v}=l_p^{1/3}v$. The force between the linkers is computed, as before, by connecting the ends of the chain into a loop of length L and computing the derivative of the total energy with respect to D. This produces

$$f(D)\approx-\frac{2k_BT}{D}+2\kappa\frac{v_a^2+v_b^2+v_av_b}{D^2}, \tag{44}$$

assuming again $L\gg D$. The first term has the form of the Casimir interaction that we obtained earlier. The second term is the elastic energy of the section of the chain between the linkers. The combined expression has a stable minimum at $f(D^*)=0$ with a separation $D^*=l_p(v_a^2+v_b^2+v_av_b)$ that is of the order of the persistence length.

One must now specify how the sliding linker molecules impose angular restrictions on the filaments to which they are bound. There are two particular cases of interest related to cross-linked F-actin networks. Some linkers that promote filament bundling, such as α-actinin, have a strong preference for parallel filaments, but others, such as the network-forming filamin cross-linkers, do not appear to generate strong angular constraints. It is simple to examine both cases if the linker molecules apply a harmonic restoring torque on the two filaments towards parallel alignment. In that case, two final Gaussian integrals remain to be done to perform a thermal average of the classical partition function over different linker angles:

$$\mathcal{Z}_{\rm cl}=\int_{-\infty}^{\infty}\frac{dv_a}{\Delta v_a}\frac{dv_b}{\Delta v_b}\exp\left\{-\frac{2l_p}{D}\left(v_a^2+v_b^2+v_av_b\right)\right\} \times\exp\left\{-\frac{\beta\gamma}{2}\left(v_a^2+v_b^2\right)\right\}, \tag{45}$$

where γ is a measure of the angular rigidity of the linker. The associated free energy is

$$\frac{\mathcal{F}_{\rm cl}(D)}{k_BT} = \frac{1}{2}\ln\left\{\frac{1}{2}(l_p/D)^2[12+8\beta\gamma D/l_p+(\beta\gamma D/l_p)^2]\right\} + C. \quad (46)$$

This expression must replace the second term in Eq. (43).

A. Network linkers

For the case that the linker molecule has little or no angular preference, we take the limit of $\beta\gamma \ll l_p/D$ and find the total force to be

$$f(D) \approx -\frac{k_BT}{D}. \quad (47)$$

The thermal average over the repulsive classical interaction simply canceled one-half of the Casimir force. The net force remains attractive as long as $\beta\gamma \ll l_p/D$. For very large separations, this condition fails. The attraction starts to increase even more and is better described by the opposite limit of bundling linkers, which have a strong angular preference. Relaxing the angle condition in going from the result given by Eq. (44) to the one given by Eq. (47) removes precisely half of the interaction strength. One may view the attraction in Eq. (44) as arising in equal parts from the restriction of two separate degrees of freedom: the position and slopes of the filament at the pinning sites. Alternatively, if one were to consider the unphysical case of cross-linkers that pin the slopes but not the positions of the filaments, one should expect the same result as in Eq. (47). More importantly, one may consider the case of cross-linkers with no angular preference and some intrinsic elastic compliance, modeled by a harmonic spring with spring constant k. Based on our results for the cross-linkers that generate a harmonic potential with curvature γ for the filament slope, we expect that the prefactor of unity in Eq. (47) would be reduced monotonically for elastically compliant cross-linkers and go to zero as $k \to 0$.

B. Bundling linkers

For the case that the linker molecule has a strong angular preference for parallel alignment, we should take the opposite limit of $\beta\gamma \gg l_p/D$. This gives

$$f(D) \approx -2\frac{k_BT}{D}\left(1-2\frac{k_BTl_p}{\gamma D}+\cdots\right) \quad (48)$$

for the total force. The repulsive interaction amounts to a small reduction of the Casimir force. The Casimir force is thus roughly twice as strong for bundle linkers than for network linkers. In the limit $\gamma \to \infty$ the final result for the Casimir force obtained from the correct evaluation of the path integral is identical to that obtained by the naive approach and subtraction scheme discussed in Sec. II B. The naive approach to the calculation of the free energy of the pinned filament introduces errors in its dependence upon the short-distance cutoff ϵ. However, by taking a derivative with respect to the inter-cross-linker spacing and subtracting the remaining formally divergent part of the resultant force as described after Eq. (18), one can mask the deficiencies of the naive approach. Other derivatives of the free energy, such as the specific heat, still retain the unphysical dependence of the naive free energy upon ϵ, as discussed after Eq. (41).

C. Effect of tension

Next consider the case that the nonzero filament tension. Rewriting the earlier results in terms of the unscaled variables, introducing the dimensionless quantity $d \equiv \sqrt{\frac{\beta\tau}{l_p}}D = \sqrt{\frac{\tau}{\kappa}}D$, and further setting the slopes $v_a = v_b = 0$ to focus on the fluctuation contribution ($\mathcal{H}_{\rm cl} = 0$), we find the free energy

$$\mathcal{F} = -k_BT\left[\ln\left(\frac{1}{D^2}\right)+\ln[W(d)]\right]+C, \quad (49)$$

where

$$W(d) = \frac{d^2}{\sqrt{2[1-\cosh(d)]+d\sinh(d)}} \quad (50)$$

is a scale function. The function $f(d)$ contains the entire correction to the free energy due to tension, which enters only through the length $\sqrt{\frac{\kappa}{\tau}}$. The force between the two linker molecules, obtained as before, is

$$f(D) = k_BT\left[-\frac{2}{D}+\sqrt{\frac{\tau}{\kappa}}\left(\frac{W'(d)}{W(d)}+\frac{1}{2}\right)\right]. \quad (51)$$

The factor $1/2$ in the second term is the contribution to the force due to filament fluctuations of chain material that is not between the two linkers. The second term is strictly positive so that the inclusion of tension weakens fluctuation attraction. For $d \gg 1$, $\frac{W'(d)}{W(d)} \approx -\frac{1}{2}+\frac{3}{2d}$. In that case, the total force is

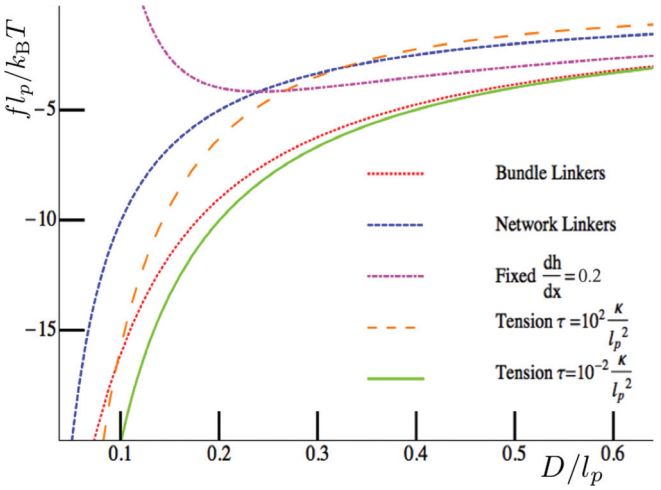

FIG. 4. (Color online) Casimir force versus cross-linker separation for a filament fluctuating in one transverse dimension. We compare the interaction in the tension-free case for network cross-linkers, which do not constrain the filament crossing angles (blue short-dashed line), and angle-constraining bundle cross-linkers (red dotted line) with zero preferred slope. When the bundle cross-linkers enforce filament slopes that introduce a nonzero mean torque (pink dot-dashed line), the interaction becomes repulsive at short distances due to the forced bending of the filament. The effect of finite tension is explored for the case of fixed tangent angles of zero at the cross-links. Increased tension reduces the attractive interaction at lengths greater than $\sqrt{\kappa/\tau}$, as can be seen by comparing the low-tension (green solid line) and high-tension (orange long-dashed line) results.

$f(D) \approx -k_B T \frac{1}{2D}$. The tension-induced fluctuation repulsion thus cancels $3/2$ of the tension-free Casimir force.

For $d \ll 1$, in contrast, the second term contributes a repulsive force that is independent of D and equal to $\frac{k_B T}{2}\sqrt{\frac{\beta\tau}{l_p}}$, but this is small compared to the tension-free fluctuation attraction. For distances small compared to the tension scale $1/q$ the full Casimir attraction is recovered. In summary, the Casimir force is not suppressed by tension for the case of bundle linkers with strongly preferred alignment. If slope fluctuations are included one finds a reduction of $k_B T \frac{1}{D}$ in the attractive force for $d \ll 1$, again illustrating that tension has no effect for distances less than the tension scale. For long distances the slope fluctuations are strongly suppressed and do not weaken the Casimir attraction. We plot the Casimir force between cross-linkers of the bundling and network types and explore the effect of tension applied to the filament in Fig. 4.

IV. CONCLUSION

We showed in this paper that when semiflexible polymers are connected by sliding linkers as in Fig. 2, then thermal conformational fluctuations generate a long-range Casimir attractive pair interaction $V(D) = \gamma k_B T \ln D$ between linkers separated by a distance D. The proportionality constant γ is a number that ranges from $1/2$ to 4 depending on (i) the presence or absence of tension along the polymer, (ii) whether or not the polymers are confined to a plane, and (iii) the rigidity of angular constraints imposed by the sliding linkers.

For distances long compared to the persistence length, the polymers can be treated as flexible. In that case, $V(D)$ can be roughly approximated as the entropic energy cost of a loop of size D, if we reinterpret D as the total polymer length between the two linkers. In that limit, the linker pair interaction maintains the same form, though the prefactor γ will be different (for non-self-avoiding polymers, γ would equal $d/2$ with d the spatial dimension). It is important to stress that the Casimir attraction between sliding linkers only is important if elastic stress does not prevent the two linkers from approaching each other. For example, if the two sliding linkers in Fig. 2 impose a nonzero angle then this generates an elastic stress that amounts to a repulsive interaction that overwhelms the Casimir interaction on length scales short compared to the persistence length. The most interesting examples of polymer networks held together by transient linkers involve F-actin filaments in the presence of linker proteins. F-actin has a persistence length in the range of 20 μm. The force between two sliding linker proteins separated by a distance of $\sim$10 nm is in the piconewton range, which is the same order of magnitude as typical forces exerted on proteins.

Any elastic compliance in the cross-linkers will decrease the overall prefactor of the Casimir interaction between them. We analyzed this effect for the case of replacing the fixed angle boundary conditions with a harmonic potential having a minimum at the desired crossing angle of the two filaments at the cross-linker. As the curvature of that potential was reduced, the contribution to the Casimir interaction coming from the pinning of the angular degrees of freedom vanished continuously. Since slope and position variables are treated analogously within the path integral formulation, replacing the boundary condition of the fixed filament position at the cross-linkers with a harmonic potential at those positions will have a similar effect. Alternately, one might consider treating the cross-linkers as small rings of radius a, as represented in our figures. If that radius is finite then undulatory modes of the filaments with an equilibrium amplitude less than a should be essentially unaffected by the rings and not contribute to the Casimir interaction. As the persistence length of the filaments diverges and all undulatory mode amplitudes decrease, the Casimir interaction must vanish. We pursued our calculation by first taking the limit of an infinitesimal ring so that our results show a finite Casimir interaction for arbitrarily long (but finite) persistence lengths. As mentioned above, however, one can still explore the effect of softening the position boundary condition by treating the cross-linker as a spring instead of a hard constraint.

Different values for γ may lead to different equilibrium phase behavior for networks of semiflexible polymers. Assume a stress-free network of semiflexible polymers held together by sliding linkers. If two neighboring linkers of a given polymer can approach each other, without generating elastic stress, then the equilibrium probability distribution $P(D)$ for the separation of the two linkers would be proportional to $\exp[-\beta V(D)] \propto 1/D^{\gamma}$. The mean square separation $\langle D^2 \rangle$ of the two linkers then would be infinite for γ less than or equal to 3. That would suggest that for γ greater than 3, linkers would come together into pairs of linkers. Would this trigger decomposition of the network as a whole? Estimate the free energy density of the linker many-body system as $F(\rho)/k_B T \approx \rho \ln \rho - (z/2d)\gamma\rho \ln \rho$, with z the average number of nearest neighbors per linker in the network and $\rho \approx 1/D^d$ the linker density. The critical value for γ above which the free energy density is a concave function of the density is $2d/z$. For larger values of γ, the network state is thermodynamically unstable. These arguments assumed that the Casimir force could be treated as a pair interaction. In Appendix B we show that this is not quite right: Three-body Casimir interactions cannot be neglected in general. The investigation of the thermodynamical stability of these networks is beyond the scope of the present paper.

We conclude by noting an important difference between the Casimir interactions in liquid membranes and on semiflexible polymers. It is essential to recognize that the linkers in our problem constrain the filament's position with respect to the space in which the filament is embedded. In other words, the filament can exchange momentum with the background system, e.g., a polymer network with the linkers at those points. If it were not constrained in this manner, so that the linker polymer system could collectively diffuse in the space, there would be no fluctuation-induced interaction between the linkers. This is demonstrated in Appendix A. This aspect of the Casimir interaction on one-dimensional elastic objects is surprising when compared to the analogous problem of rigid, disklike inclusions in an isolated membrane. These are known to interact via a power-law Casimir force even if the collective disk and membrane system were allowed to freely diffuse in the embedding space. One cannot simply generalize this membrane result to the semiflexible polymer problem and this has significant biophysical implications. Based on our result, we predict that DNA binding proteins do not

experience a long-range attractive Casimir interaction along a DNA filament, while membrane-bound proteins do.

ACKNOWLEDGMENTS

R.B. would like to thank the NSF for support under Grant No. NSF-DMR-1006128. A.J.L. thanks the NSF for support under Grant No. NSF-DMR-1006162. We especially thank E. D'Hoker for fruitful conversations on the quantum Casimir problem.

APPENDIX A: NO CASIMIR INTERACTION FOR RIGID INCLUSIONS WITHIN THE SPIN-WAVE APPROXIMATION

Consider a free semiflexible filament fluctuating in the plane with two linkers attached. The Hamiltonian for the filament, parametrized by the angle of the local tangent with respect to a reference direction $\theta(s)$ as function of arc length, is given in the usual form

$$\mathcal{H}\{\theta(s)\} = \frac{1}{2}\int_0^L ds\,\kappa(s)\left(\frac{d\theta}{ds}\right)^2. \tag{A1}$$

The role of the attached linkers is to modify the local bending stiffness of the filament $\kappa(s)$; the filament has one bending modulus at the linkers' locations and another elsewhere. The partition function for such a system may be written as

$$\mathcal{Z} = \int \mathcal{D}\theta\, e^{-\beta\mathcal{H}\{\theta(s)\}}. \tag{A2}$$

The above partition function is that of the one-dimensional nonlinear σ model, but with a nonuniform stiffness. The functional integration should respect the restriction of $\theta(s)$ to the unit circle: $0 \leqslant \theta < 2\pi$. In the case of interest where the entire chain segment is much shorter than a persistence length, the partition sum is dominated by a small range of tangent angles so that this constraint can be neglected. Having done so, we perform the functional integral over $\theta(s)$, treating it as a Gaussian variable. In the nonlinear σ model, this is known as the spin-wave approximation. Discretizing the functional integral again in chain segments of length ϵ and assuming periodic boundary conditions, we obtain

$$\mathcal{Z} = \left[\prod_{n=1}^{N}\int_{-\infty}^{\infty}\frac{d\theta_n}{\Delta}\right]\exp\left\{-\frac{1}{2\epsilon}\sum_{n=1}^{N}\beta\kappa_n(\theta_{n+1}-\theta_n)^2\right\}, \tag{A3}$$

with $\theta_{N+1} = \theta_1$. Since there are no higher-order derivatives, there are no ambiguities of the kind previously discussed in the evaluation of the functional integral. Introducing the difference variable $y_n = \theta_{n+1} - \theta_n$ and performing the Gaussian integrals, we arrive at

$$\mathcal{Z} \propto \prod_{n=1}^{N}\frac{1}{\sqrt{\beta\kappa_n}}. \tag{A4}$$

It is evident from this expression that the partition function does not depend on the separation of the two beads on the filament; there is no fluctuation-mediated interaction between the beads within the spin-wave approximation.

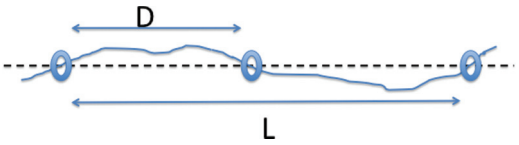

FIG. 5. (Color online) Three interacting sliding linkers on a single fluctuating filament.

APPENDIX B: THREE-PARTICLE INTERACTION

Consider three sliding linkers on a fluctuating filament as shown in Fig. 5. The classical and Casimir contributions to the free energy in a tensionless filament in the scaled units are

$$\mathcal{F} = 2k_BT\left(\ln\tilde{D} + \ln(\tilde{L}-\tilde{D}) + \frac{\tilde{v}_a^2+\tilde{v}_b^2+\tilde{v}_a\tilde{v}_b}{\tilde{D}} + \frac{\tilde{v}_b^2+\tilde{v}_c^2+\tilde{v}_b\tilde{v}_c}{\tilde{L}-\tilde{D}}\right). \tag{B1}$$

If one assumes that the linkers have no angular preference then the $\tilde{v}_i$ may be integrated out and one finds the interaction free energy

$$\mathcal{F} = k_BT\left[\ln\tilde{D} + \ln(\tilde{L}-\tilde{D}) + \tfrac{1}{2}\ln\tilde{L}\right]. \tag{B2}$$

The Casimir force on the middle linker is

$$f = -k_BT\left(\frac{1}{\tilde{D}} - \frac{1}{2(\tilde{L}-\tilde{D})}\right). \tag{B3}$$

The force on the leftmost linker is

$$f = -k_BT\left(\frac{1}{\tilde{D}} + \frac{1}{2\tilde{L}}\right). \tag{B4}$$

As we let $\tilde{D} \to \tilde{L}$ corresponding to a single linker interacting with a cluster of two linkers we see the force goes to $-\frac{3k_BT}{2\tilde{L}}$. This result highlights the fact that tight clusters must eliminate fluctuations and therefore force the slopes to be identically zero at the edges of the cluster. Fluctuating slopes generate repulsive forces of strength $-\frac{k_BT}{2\tilde{L}}$, so the elimination of such fluctuations increases the overall strength of the attraction. We see that an individual linker will be preferentially attracted to clusters over solitary linkers. This result holds for the interaction of a single linker with any size cluster up to correction of order $\frac{a}{L}$, where a is the mean spacing within a cluster and L is the separation of the single linker with the cluster. We may also deduce that two clusters will interact with the full fluctuation force $-\frac{2k_BT}{\tilde{L}}$ since there are no slope fluctuations at either end.

APPENDIX C: SEMIFLEXIBBLE FILAMENT EQUILIBRIUM FLUCTUATIONS

In this Appendix we address the questions of the overall scale of the transverse fluctuations of a filament in order to demonstrate that the thermally generated undulations are sufficiently large so as to be affected by cross-linkers that imperfectly pin the filament, such as ring cross-linkers shown schematically in Figs. 2 and 5. To do this we consider a filament of length $L \ll l_p$ without applied tension. In this case the

energy of a given deformation $h(z)$ is

$$E = \frac{\kappa}{2}\int dz\left[\partial_z^2 h(z)\right]^2. \tag{C1}$$

We take the filament to be hinged at $z = 0$ and free at $z = L$ and determine the characteristic fluctuations a distance l from $z = 0$. The boundary conditions are then $h(0) = h'(0) = 0$ and $h''(L) = h'''(L) = 0$, where primes denote differentiation with respect to z. For these boundary conditions we may integrate by parts to get

$$E = \frac{\kappa}{2}\int dz\, h\partial_z^4 h. \tag{C2}$$

To determine the thermal expectation value of the filament's transverse displacement at $z = l$ it is convenient to decompose those displacements into eigenfunctions of the ∂_z^4 operator with the boundary conditions imposed above. These are

$$h_n = c_n\left[\sin(k_n z) + \frac{\sin(k_n L)}{\sinh(k_n L)}\sinh(k_n z)\right], \tag{C3}$$

with corresponding eigenvalue k_n^4, where k_n are the solutions of the transcendental equation

$$\tan(k_n L) = \tanh(k_n L) \tag{C4}$$

and c_n is a normalization constant chosen so that

$$\int_0^L dz\, h_n^2(z) = 1. \tag{C5}$$

We further simplify the analysis by considering only the first mode $n = 1$. Since the mean square amplitudes of each mode are positive-definite quantities that add to the quantity of interest $\langle h^2(l)\rangle$, our result provides a conservative underestimate of the rms fluctuations of the filament.

From the equipartition theorem

$$\frac{\kappa}{2}\langle A_1^2\rangle k_1^4 = \frac{k_B T}{2}, \tag{C6}$$

where A_1 is the amplitude of the first mode. The local height fluctuations are then given by

$$\langle h^2(l)\rangle = \frac{k_B T}{\kappa k_1^4(L)} h_1^2(l;L) + \cdots, \tag{C7}$$

where we note explicitly the dependence of the eigenfunction and eigenvalue on the filament's length L. The ellipsis represents positive terms associated with the neglected modes. The eigenfunction scales as $h_1(l;L) \sim L^{-1/2}k_1 l$ due to the normalization factor c_1 of the eigenfunction and its dependence on l for small l. The eigenvalues scale as $k_1 \sim L^{-1}$, so $h_1(l;L) \sim L^{-3/2}l$. Combining this with Eq. (C7) and recalling that $l_p = \kappa/k_B T$, we find

$$\langle h^2(l)\rangle \sim \frac{l^2 L}{l_p}. \tag{C8}$$

The rms fluctuations are then estimated to be $\sqrt{\langle h^2(l)\rangle} \sim l\sqrt{L/l_p}$. Taking parameters appropriate for a 1-μm filament of F-actin ($l_p \sim 10\ \mu$m), we find that

$$\sqrt{\langle h^2(l)\rangle} = 0.1l. \tag{C9}$$

At a separation of $l = 100$ nm the fluctuations are approximately 10 nm. If we imagine that the hinged boundary condition at $z = 0$ is due to a cross-linker with no angular preference then we expect to have a meaningful Casimir interaction at a separation of 100 nm since a physical cross-linker should be capable of constraining fluctuations of order 10 nm. Assuming cross-linkers can affect fluctuations on the scale of 1 nm, we arrive at our estimate for the short-distance cutoff for Casimir interactions between physical cross-linkers: separations of 10 nm. This result is somewhat sensitive to boundary conditions: A clamped boundary condition at $z = 0$ leads to a quadratic growth profile and would produce fluctuations of only a few nanometers at $l = 100$ nm and thus extend our short-distance cutoff of the Casimir interaction to such a distance.

[1] H. B. G. Casimir, Proc. K. Ned. Akad. Wet. **51**, 793 (1948).
[2] S. Weinberg, Rev. Mod. Phys. **61**, 1 (1989).
[3] E. D'Hoker and P. Sikivie, Phys. Rev. Lett. **71**, 1136 (1993).
[4] A. Ajdari, B. Duplantier, D. Hone, L. Peliti, and J. Prost, J. Phys. II France **2**, 487 (1992).
[5] M. Krech, *The Casimir Effect in Critical Systems* (World Scientific, Singapore, 1994).
[6] V. Mostepanenko and N. N. Trunov, *The Casimir Effect and Its Applications* (Oxford University Press, Oxford, 1997).
[7] M. Kardar and R. Golestanian, Rev. Mod. Phys. **71**, 1233 (1999).
[8] R. Bruinsma, M. Goulian, and P. Pincus, Biophys. J. **67**, 746 (1994).
[9] P. Ziherl, R. Podgornik, and S. Žumer, Chem. Phys. Lett. **295**, 99 (1998).
[10] M. Doi and S. Edwards, *The Theory of Polymer Dynamics* (Clarendon, Oxford, 1986).
[11] M. Rubenstein and R. Colby, *Polymer Physics* (Clarendon, Oxford, 2003).
[12] H. Kleinert, J. Math. Phys. **27**, 3003 (1986).
[13] H. Yamakawa and M. Fujii, Chem. Phys. **59**, 6641 (1973).
[14] F. Gittes, B. Mickey, J. Nettleton, and J. Howard, J. Cell Biol. **120**, 923 (1993).
[15] L. D. Landau and E. M. Lifshitz, *Theory of Elasticity* (Pergamon, New York, 1986).
[16] C. Bustamante, J. Marko, E. D. Siggia, and S. Smith, Science **265**, 1599 (1994).
[17] H. Kleinert, *Path Integrals in Quantum Mechanics, Statistics, Polymer Physics, and Financial Markets* (World Scientific, Singapore, 2010).
[18] I. S. Gradshteyn and I. M. Ryzhik, *Table of Integrals, Series, and Products* (Academic, New York, 1994).